

Opal-A and associated microbes from Wairakei, New Zealand: the first 300 days

B. Y. SMITH¹*, S. J. TURNER² AND K. A. RODGERS³

¹ Department of Geology, University of Auckland, Private Bag 92019, Auckland, New Zealand

² School of Biological Sciences, University of Auckland, Private Bag 92019, Auckland, New Zealand

³ Research Associate, Australian Museum, Sydney, NSW 2000, Australia

ABSTRACT

All samples of silica sinter, <2 y old taken from the discharge drain of the Wairakei geothermal power station and the Rainbow Terrace of Orakei Korako, consist of non-crystalline opal-A. This silica phase deposits directly upon the concrete drain wall and filamentous templets, extending from this wall, afforded by the microbial community present in the drain, whose nature was determined by a culture-independent strategy that entailed construction, fingerprinting and sequencing of a 16S clone library. The bacterial community is dominated by five major groups of organisms, present in approximately equal proportions, and which account for ~50% of the community. None of the 16S sequences from these dominant groups yielded a perfect match with 16S sequences for named organisms in the international databases. However one dominant group clusters with *Hydrogenophilus thermoluteus*, a thermophilic filamentous bacterium, and two cluster with putatively thermophilic members of the *Cyanobacteria* and green non-sulphur bacteria respectively. Initial opal-A deposits rapidly as agglomerations of silica nanospheres that, in turn, form chains of coalesced, oblate, microspheres <0.4 × 0.2 μm about the barbicel-like filaments, to produce a mat of fine woven strands. The majority of individual filaments are <8 μm long and 0.8 μm wide but may be up to 55 μm long by 1 μm wide. Where laminar flow dominates, most strands develop parallel to the drain current but some strands crisscross while others protrude above the mat surface. Where flow is turbulent, strands lack preferred orientation and some adopt a helical form. In general, following deposition, the values of the scattering broadband at half (FWHM) and three quarters (FWTM) of the maximum intensity decrease with increasing sample age. The behaviour of the band at one quarter maximum intensity (FWQM) is less consistent, but, in general, the youngest sinters possess the highest FWQM, FWHM and FWTM values that prove independent of fabric type. Opal-A silica matures following its removal from the parent fluid, especially where the sinter surface is filmed by water. A continual movement of silica is shown by a second generation of microspheres formed on the silica mat surface, by an increase in size of the initial microspheres, and by an increase in maximum intensity of the X-ray scattering broadbands. Similar silica aging behaviour occurs among young sinters developed upon microbial mats at Orakei Korako. The deposition and aging processes accord with the known behaviour of juvenile opaline silica in both natural and artificial systems whose pH, temperature and dissolved salt content are similar to Wairakei and Rainbow terrace: gelling of silica is favoured by the high pH (~8.3) and temperature (~60°C) of the Wairakei discharge fluid but the high dissolved salt content of the water (Na⁺ = 930 μg/g, Ca²⁺ = 12 μg/g, Cl = 1500 μg/g) and abundant microbial community facilitate rapid and copious flocculation of solid silica within the drain, in contrast to the slower accumulation on the natural sinter terrace at lower temperature (30–45°C) from less saline dilute bicarbonate-chloride waters (Na⁺ = 180 μg/g, Ca²⁺ = 0.2 μg/g, Cl = 400 μg/g, pH = 8.1).

KEYWORDS: sinter, Wairakei, New Zealand, bacterial community, microbes.

* E-mail: gbijsmith@kiwilink.co.nz

DOI: 10.1180/0026461036730118

Introduction

WHEN first deposited, sinter from near-neutral alkali chloride waters consists of opal-A, a non-crystalline, hydrated silica phase (Smith, 1998; Herdianita *et al.*, 2000a). While all materials that come in contact with discharging thermal waters, be they biogenic or abiogenic, can afford a potential substrate for the coagulating silica, it has long been known that microbes such as the Cyanobacteria and *Archaea* that thrive in the hot spring environments, are particularly effective at mediating the deposition of the opaline silica (e.g. Weed, 1889a,b). The silica flocculates upon and about the different microbial templates to produce moulds of the filaments with a range of distinctive textures that have become the focus of particular interest in recent years (e.g. Cady and Farmer, 1996; Farmer, 2000).

The nature of the microbial communities involved in the silica sinter depositional process and the mechanisms of microbe-mediated silicification are, as yet, unclear. Much of our lack of understanding has stemmed from our inability to culture, and hence identify and study *in vitro*, the vast majority of environmentally associated microbes. The recent development of culture-independent molecular methods provides a solution to this problem by enabling the nature of microbial communities to be determined from bacterial DNA extracted directly from environmental samples (Amann *et al.*, 1995). 16S ribosomal RNA (rRNA) genes are a useful target for these analyses as they are highly conserved, being found in all microorganisms, while also containing variable sequence regions, or signature sequences, that enable taxonomic classification organisms to the level of species. Comparative DNA sequence analysis of 16S genes is now widely used for the characterization of complex microbial communities and for the taxonomic description of microorganisms from a broad diversity of environments including subsurface scale at the Otake geothermal power station, Japan (Inagaki *et al.*, 1997) and Yellowstone hot spring communities (Blank *et al.*, 1999; Hugenholtz *et al.*, 1998; Inagaki *et al.*, 2001).

At the Wairakei geothermal power station, New Zealand (Fig. 1), the discharge drain contains both an extensive microbial community and an unlimited supply of fresh opal-A. Consequently, the opportunity exists to analyse both the nature and diversity of a microbial community, and the initial silica depositing amongst that community.

The results presented here constitute a first step towards obtaining a total picture of the singular and intimate character of the primary microbe-mineral connection in the first days of silica deposition.

Following deposition upon the microbial substrate, Herdianita *et al.* (2000a) demonstrated that changes occur in both the physical properties and in the textures of the opal-A silica phase, such that the primary depositional textures, including any bacterial templates, are modified to varying degrees. Ultimately, opal-A transforms with time into paracrystalline opal-CT and/or opal-C, and, subsequently, to microcrystalline quartz. The maturation process typically takes ~50,000 y for Taupo Volcanic Zone (TVZ) sinters.

In order to appraise fossil textures it is essential to understand the manner and extent of any modifications an opal-A mould may undergo. While Herdianita's *et al.* (2000a) model of sinter aging is helpful in this respect, all samples of opal-A with an age of ≤ 1 y were plotted by these authors on a single, year-1 time line, i.e. no indication was given as to whether changes occurred in the physical character of opal-A during its first year. In point of fact, they recorded a range of values in the properties of their year-1 samples that is greater than any seen among samples a few years old.

Given that a supply of older sinter, available at Wairakei, was deposited in distinct time brackets over previous months, the opportunity was also taken to investigate whether the spread of values observed by Herdianita *et al.* (2000a) reflects mineralogical processes initiated immediately upon or soon after deposition, following the entombment and silicification of the bacterial precursors, i.e. what changes, if any, occur in opaline silica immediately following deposition.

Samples with numbers prefixed AU are held in the Department of Geology, University of Auckland Petrology Collection.

Sample occurrence

Samples are categorized into 3 groups (Table 1).

Group A

Thick deposits, typical of streamer microfacies silica, accumulate at a rate of a few hundred mm/y in the drains used to discharge waste water from the Wairakei geothermal power station. These drains consist of two adjoining concrete channels each 1.5 m wide. The build up of silica is such

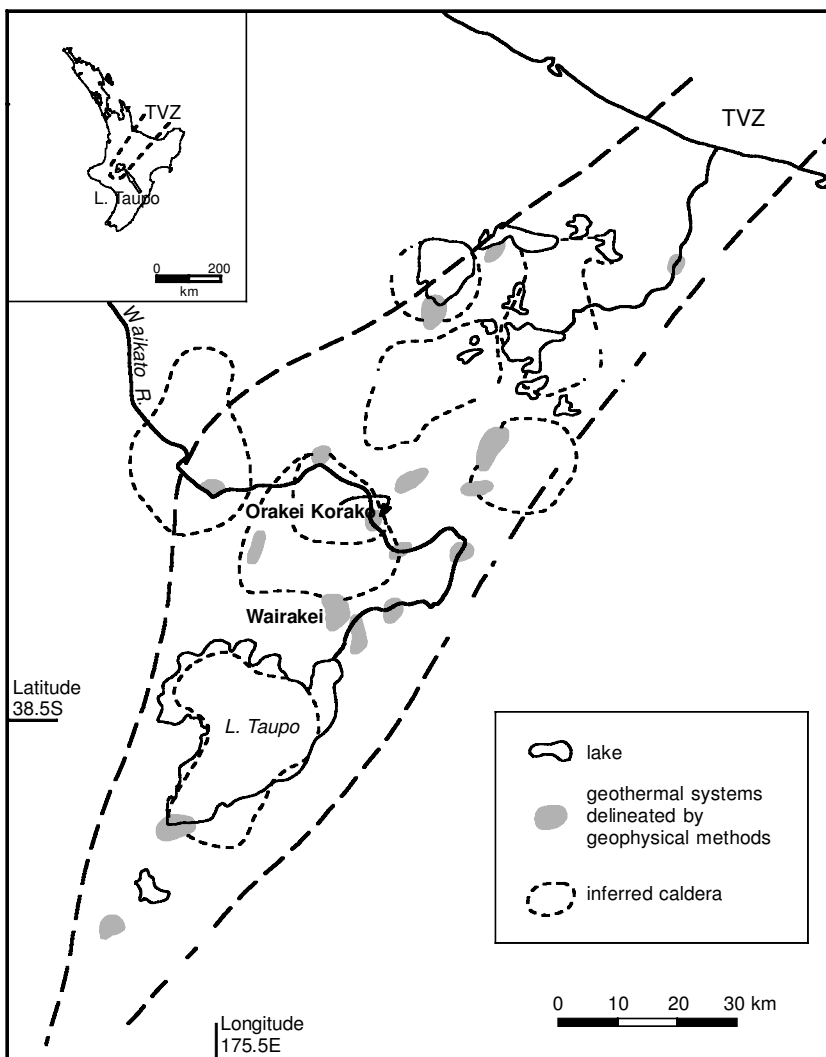


FIG. 1. Sketch map, showing the locations of Wairakei and Orakei Korako geothermal fields within the Taupo Volcanic Zone. Insert: North Island, New Zealand.

that the drains become clogged and require cleaning every six months or so. A central divider separates the channels and was originally intended to permit each to be used independently but ground subsidence has caused the hot discharge water level to overtop this divider and it has become a primary site for sinter deposition (Fig. 2). Flow rate is currently ~500 l/s with water cooling from 95°C at input to ~60°C immediately above a major drop structure.

The resulting, silica-coated, streamers possess an underlying habit that resembles the structure of

feathers. An elongate strand or group of strands forms a central shaft or rachis that can commonly grow up to 50 mm in length. From this, numerous barb-like strands, commonly 5–10 mm long, divaricate. In turn, these subdivide to produce even smaller barbicel-like filaments, up to 55 µm long, that interlock in a manner akin to the barbicel hooks of feathers. Unlike feathers, however, the diameters of silica-coated rachis, barbs and barbicels are similar.

For DNA analysis, sinter samples were collected which comprised the growing tips of

TABLE 1. Representative opal-A scattering band parameters of silica from young sinters of Wairakei and Orakei Korako, New Zealand.

Group	Age (y)	Age (days)	Location	AU no ¹	Max. intensity (c/s)	Position of max. intensity (Å)	FWQM ΔÅ	FWHM ΔÅ	FWTM ΔÅ
A	≤0.12	<46	Wairakei drain	52387_6h	93	3.99	2.23	1.37	0.80
	≤0.13	<49		52387_3d	90	4.00	2.10	1.29	0.75
	≤0.14	<51		52387_5d	94	3.95	2.17	1.33	0.77
	≤0.16	<62		52387_16d	90	3.98	2.20	1.39	0.79
	≤0.20	<73		52387_37d	92	3.97	2.20	1.34	0.79
≤0.29	<106	52387_60d	114	4.02	2.13	1.33	0.71		
B	≤0.4	<<<234	Ex Wairakei drain	52388b	103	3.93	2.20	1.33	0.84
	≤0.4	<<<234		522388a	97	3.99	2.23	1.35	0.79
	≤0.5	<<234		52389b	103	3.95	2.10	1.32	0.84
	≤0.6	<234		52389a	90	3.94	2.23	1.32	0.68
C	<0.25		Orakei Korako	52391	102	4.00	2.16	1.40	0.80
	<0.5			52396a	104	3.98	2.13	1.39	0.81
	<1			52392a	106	4.00	2.14	1.30	0.72
	~1			52392b	112	4.02	2.04	1.25	0.72
	>1 and <2			52394	107	3.99	2.03	1.30	0.76
	<2			52393	110	3.97	1.98	1.30	0.77

¹ h = hours; d = days

fresh, well-developed streamer microfacies deposited on the central divider. Samples were placed in 15 ml sterile polypropylene tubes, stored at 4°C overnight and then transferred to -20°C storage pending further analysis. A larger sample of the same material was taken for mineralogical analysis (sample AU52387). Immediately following collection, this sample was placed in a clean container, filled with the parental discharge water, which, at the time of sample collection, had a temperature of 62.5°C and a pH of 8.3. Subsequently, subsamples were removed from the water and air dried at room temperature for differing periods. These intervals are denoted by the numerical suffix attached to the sample number e.g. _6h = 6 hours, _3d = 3 days, and represent time elapsed following removal from the parent fluid. A minimum of six hours was needed to air dry the sample sufficiently for mineralogical analysis and this initial subsample, AU52387_6h, has been taken as the benchmark of fresh, unaltered silica sinter for the purposes of this study.

All Group A samples were very young, particularly given that the drain had been cleaned out <6 weeks earlier (R. Smith, pers. comm.) As such, the maximum time that could

have elapsed since deposition is 42 days although it seems likely that the tips, at least, of the collected sample may be no more than a few days old. Four days elapsed between removing the mineralogical sample from the drain and its initial physical analysis.

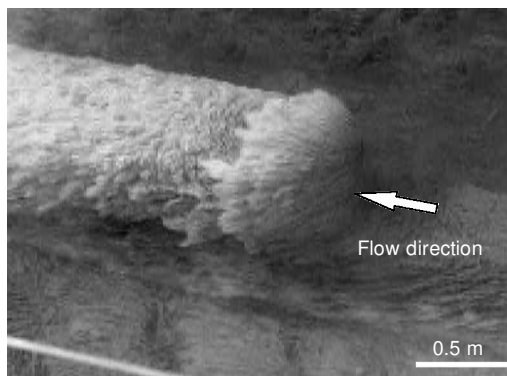


FIG. 2. Silica sinter, displaying streamer fabric, actively depositing upon the central divider of the Wairakei discharge drain.

Group B

Sinter samples from the last clearing of the drain, 6 weeks earlier, were collected from the adjacent bank. All consisted of massive streamer microfacies scraped from the walls of the discharge sluice. These samples are identical in all respects to group A except they were formed at an earlier date and have been subject to slight weathering. Given that the second most recent cleaning of the drain had occurred 6 months previously, the maximum possible depositional age of any of these older samples, at the time of analysis, was 234 days. Sample AU52389 exhibits a zonal structure. The zone deposited immediately adjacent to the drain wall (AU52389a, zone 1) has been assigned an age of <0.6 y, the maximum time elapsed from deposition. By definition the outer (drainward) zones are younger and the next layer drainwards (AU52389b, zone 2) was taken as having an arbitrary age of <0.5 y. Two additional samples, AU52388a and AU52388b, both exhibit well developed streamer fabric and show no evidence of having been formed adjacent to the wall. They are taken, subjectively, as having ages of <0.4 y.

Group C

The Wairakei drain specimens fail to provide a total overlap in age with those examined by Herdianita *et al.* (2000a). In order to confirm and more fully explore the nature and extent of trends observed in the physical properties of the Wairakei silica following its deposition, a number of additional examples of young, naturally occurring silica sinter were taken from the large sinter terraces of Orakei Korako, an active geothermal field situated some 18 km north-northeast of Wairakei in the Taupo Volcanic Zone (Fig. 1; Lloyd, 1972). No DNA analyses were undertaken of any of these specimens. Sinter accumulation rates from the dilute bicarbonate-chloride water discharging at Orakei Korako are markedly lower than at Wairakei and vary from a high of 25 mm/y about Hochstetter's Pool to an annual average of ~1 mm/y at Golden Fleece Terrace (Lloyd, 1972). Estimates of sample ages have been made, partly on these rates of sinter accumulation and, partly on the position the different samples occupied within the sinter aprons.

A complete overlap of sample ages with those from Wairakei drain was not possible as examples of very young, partly silicified

microbes from the environmentally protected Orakei Korako area all provided insufficient silica for powder X-ray diffraction (XRPD) analysis. This proved to be the case particularly in an attempt to sample very young, living streamer microfacies, AU52404. The bacterial mat had formed in a channel, 0.15 m wide and 0.04 m deep, with a water temperature of 56°C and a velocity of 0.3 m/s. All filaments were aligned with the flow direction. Similarly, a very young, living, pustular orange bubble mat, from an adjacent area, AU52390, yielded insufficient silica. This sample was growing on a mid-slope sinter apron in water 0.01 m deep, with a velocity of 0.5 m/s and a temperature of 42.3°C.

Adequate silica was obtained from somewhat older, but still young, partially silicified, filamentous cyanobacteria-like assemblages representing both bubble mat and palisade microfacies; samples AU52391 and AU52396a, respectively. Sample AU52391 came from a partially submerged pustular bubble mat growing on a mid-slope sinter apron in 45°C water, with a velocity of 0.3 m/s. The silica was taken from the silicified periphery of the mat where it seemed likely to have been deposited within the previous three months. Palisade sample AU52396a came from the lip of a channel at the top of an accumulating sinter apron and was associated with green, living, mid-temperature-sized cyanobacteria-like organisms. The water temperature was 54°C.

Older samples AU523924 from the bubble mat microfacies provide the second end-member for the present study, complementing the very fresh Wairakei drain AU52387. Samples AU52932 came from a partially submerged, totally silicified bubble mat developed on a broad sinter apron in a water temperature of 53°C. AU52392a is from the totally silicified top lamina of the silicified bubble mat formed at the air/water interface. The age of this upper exposed lamina is estimated to be >0.5 y but <1.0 y. AU52392b consists of smooth silica laminae formed immediately below AU52392a and is considered to be ~1.0 y old. Samples AU52393–4 came from dry sinter terraces and consist of smooth silica laminae formed about voids. Their age is estimated to be <2.0 y.

Importantly, none of the samples in this group had suffered overprinting from post-depositional steam heating or weathering, both of which, it was found, can affect the physical properties of young sinter.

Methods

Analysis of the microbial community in the drain sample was undertaken using a culture-independent strategy that entailed extraction of bacterial DNA from the sinter samples followed by PCR amplification, cloning, restriction fragment length polymorphism (RFLP) fingerprinting and sequencing of a 16S clone rRNA gene library. A detailed review of this and other 16S-based methods is presented in Amann *et al.* (1995). Unless otherwise stated in the summary below, molecular methods were those described in Sambrook and Russell (2001), with DNA extraction performed using a modification of a method described by Miller *et al.* (1999). Full experimental details may be obtained from one of the authors (SJT).

DNA isolation

Approximately 0.5 g of the sinter sample was weighed into a sterile 2 ml screw-cap microtube containing 0.5 g each of 0.1 mm and 3.0 mm silica-zirconium beads. Equal volumes (300 µl) of phosphate buffer (100 mM NaH₂PO₄ pH 8.0), lysis buffer (100 mM NaCl, 500 mM Tris pH 8.0, 10% SDS) and chloroform-isoamyl alcohol (24:1) were added and the tubes machine shaken vigorously (45 m/s) for 40 s. The tubes were then centrifuged at 13,100 g for 5 min and 650 µl of supernatant were recovered from which proteins and SDS were precipitated by adding of 360 µl of 7 M ammonium acetate and placing the tubes on ice for 5 min. The tubes were centrifuged at 13,100 g for 5 min and the upper aqueous phase recovered and DNA precipitated by adding 0.54 volumes of isopropanol, and centrifuging again at 13,100 g for 5 min. The supernatant was discarded and the pellet washed with 1 ml of 70% ethanol, followed by centrifugation at 13,100 g for a further 5 min. Following removal of the supernatant, the pellet was allowed to air dry for 30 min then resuspended in 100 µl of water. To improve recovery of DNA the extracts were supplemented with 2 µl of linear polyacrylamide carrier (Molecular Research Center Inc., Cincinnati OH) prior to DNA precipitation.

PCR amplification of 16S genes

Bacterial 16S rRNA gene sequences were PCR amplified from the sample DNA using universal primers PB36 (AGRGTGGATCGTGGCTCAG)

and PB38 (GKTACCTTGTTACGACTT). These primers amplify the near-full length 16S gene spanning positions 8–1509 (*E. coli* numbering: Brosius *et al.*, 1981). Samples were also screened for *Archaea* using PCR primers A16S.1 (CCAGGCCCTACGGGGCGCA) and A16S.2 (GTGTGCAAGGAGCAGGGAC). No PCR products were detected using these primers and all further analysis was centred on PCR products obtained from the bacterial primers. The PCR reactions were performed in 50 µl volumes containing 20 mM Tris-HCl pH 8.6, 50 mM KCl, 2.0 mM MgCl₂, 100 µM each dNTP, 1.0 units PlatinumTaq™ (Invitrogen Life Technologies, CA), 0.2 µM of each primer and 2.0 µl of DNA template. Amplification was carried out using a program of 94°C for 3 min followed by 25 cycles of 94°C, 45 s; 55°C, 45 s; and 72°C, 90 s. Duplicate PCR reactions were carried out on each sample. The duplicate PCR products were pooled and then purified using a High Pure PCR Purification Kit (Roche Diagnostics, Mannheim, Germany) according to the manufacturer's instructions. Negative (no DNA) and positive (seeded) controls were included to check for DNA contamination of reagents and the efficiency of PCR amplification respectively. PCR amplification products were assayed for quality and quantity by polyacrylamide gel electrophoresis (PAGE) against a Low DNA Mass Ladder (Invitrogen Life Technologies).

Clone library construction and screening

Purified PCR products were ligated into a T-tailed PCR cloning vector (pGEM-T; Promega Madison WI) essentially as described in the manufacturer's protocols. Ligation reactions were prepared in 15 µl volumes and incubated overnight at 4°C. The resulting ligation products were transfected into *E. coli* DH5α competent cells in accordance with the manufacturer's protocol with the exception that Luria broth was used instead of SOC medium. Transformants containing inserts were identified by blue-white selection on L-agar plates. A clone library of 96 randomly selected white colonies was prepared for further analysis. Individual clones were subcultured in 150 µl of L-broth in a microtitre-tray format and incubated at 37°C overnight. Crude cell lysates were prepared for PCR analysis by transferring 50 µl of the broth culture to a new tube containing 100 µl of sterile H₂O and incubating at 94°C for 20 min. Lysates were centrifuged at 3000 g for

5 min to sediment cell debris and were stored at -20°C prior to analysis. The remaining portions of the cultures were supplemented with 15% glycerol and stored at -80°C . Inserts were recovered from cell lysates by PCR amplification using vector-specific primers pGEM-F (GGCGGTGCGGGGAATTCGATT) and pGEM-R (GCCGCGAATTCAGTAGTGATT). The PCR reactions were performed in 20 μl volumes containing 20 mM Tris-HCl pH 8.6, 50 mM KCl, 2.0 mM MgCl_2 , 100 μM each dNTP, 1.0 units PlatinumTaqTM, 0.2 μM each of primers pGEM-F and pGEM-R and 1.5 μl of crude cell lysate. Amplification was carried out using the same program as described above for primers PB36 and PB38. The resulting PCR products were screened for similarity by RFLP fingerprinting using the restriction endonuclease *Hae*III. Restriction digests were performed in 25 μl volumes comprising 20 μl of PCR product, 2.5 μl of $10\times$ React 2 buffer and 5 U *Hae*III and were incubated overnight at 37°C . Digestion products were resolved by PAGE through 6% non-denaturing gels. Fingerprint profiles for the clone library were compared for similarity and each different pattern assigned an Operational Taxonomic Unit (OTU) reference number. Representative clones were randomly selected from the five dominant OTUs for DNA sequencing. Insert DNA was prepared for sequencing by PCR amplification from cell lysates as described above, with the exception that duplicate reactions were carried out in 50 μl volumes for each clone to be sequenced. The duplicate PCR products were pooled and purified using a High Pure PCR Purification Kit according to the manufacturer's instructions. The DNA sequencing was performed using dye-labelled terminators on an ABI 3100 sequencer fitted with 80 cm capillaries. Sequencing was carried out using both forward and reverse pGEM primers and an internal primer 16S.5 (GCTCGTTGCGGGACTTAACC) which enabled the sequence of the entire insert to be obtained.

Sequence editing and phylogenetic analysis

The sequence data for each clone were compiled, checked for ambiguities and edited into a full length consensus sequence using the Autoassembler computer program (ABI). Preliminary information on the phylogenetic placement of sequences was obtained by comparison with sequences in the Genbank Database

(<http://www.ncbi.nlm.nih.gov>) using the program BLAST (Altschul *et al.*, 1990).

Mineralogy

Of the different physical properties of silica sinter phases that Herdianita *et al.* (2000a) found to vary with time, the most sensitive response was in the size and shape of the X-ray scattering broadband or diffraction line centred at $\sim 4 \text{ \AA}$. The most convenient property of the opal-A scattering band used by Herdianita *et al.* (2000a,b) to compare individual specimens was the full width at half maximum (FWHM). The authors equated this measurement with the degree of lattice disorder, an approach analogous to that used to evaluate the crystallinity of some clays. The same strategy has been adopted here to appraise differences in opal-A at various stages of its aging process and to enable direct comparisons to be made with the Herdianita *et al.* (2000a) maturation model. However, in the present study it was also found useful to include measurements of full width at quarter maximum (FWQM) and full width at three quarter maximum (FWTM), along with the position and intensity of the scattering maximum above background, in order to better describe the size and shape of the different scattering bands for comparative purposes (Fig. 3).

All samples were scanned by a Philips X-ray Diffractometer fitted with a graphite monochromator with acquisition controlled by Diffraction Technology VisXRD software, using the same rigorously constrained instrumental settings and experimental conditions detailed by Herdianita *et al.* (2000b) to permit direct comparison between the present results and those of Herdianita *et al.* (2000a). Operating conditions were 40 kV at 20 mA, using Cu-K α radiation ($\lambda_{\alpha 1} = 1.5405 \text{ \AA}$). Samples of untreated, dry, hand ground, $<106 \mu\text{m}$ powders, were mounted in a $10 \times 20 \times 1.5 \text{ mm}$ aluminium holder, and scanned at $0.6^{\circ}2\theta/\text{min}$ from $10\text{--}40^{\circ}2\theta$, with a step size of 0.01° . An internal silicon standard was used from time to time to check the alignment of the diffractometer. Measurements of FWQM, FWHM and FWTM have a precision of $\pm 0.008 \Delta d \text{ \AA}$ or $\pm 0.07 \Delta 2\theta^{\circ}$ (cf. Herdianita, 2000b). The measurement repeatability of maximum intensity was no better than $\pm 2 \text{ c/s}$.

Along with the variation in physical properties, progressive changes are known to occur in the morphology of the different ultrastructural textural components of the sinter. Each of the

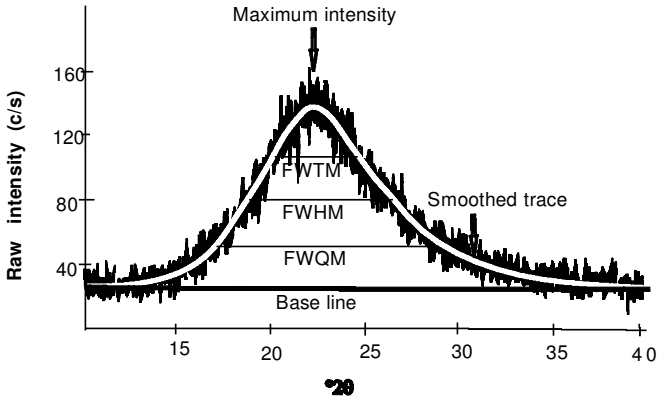


FIG. 3. Typical opal-A X-ray scattering broadband showing measurement of full width at half maximum (FWHM), quarter maximum (FWQM) and three-quarter maximum (FWTM) of smoothed trace, along with maximum scattering intensity. All measurements are made relative to a base line constructed as a tangent to the smoothed scattering trace.

samples was examined by a high resolution scanning electron microscope (SEM) to see if any consistent changes were apparent in the first year of the existence of opal-A. In addition, a cryostage was used to examine samples AU52404 and AU52390 to ascertain the relationship between the living microbial ultrastructure and initial opal-A flocculant.

Results

Microbial community analysis

A total of 72 clones from the bacterial 16S library were screened by RFLP fingerprint analysis yielding 70 unambiguous fingerprint profiles.

Discrete profiles were defined as Operational Taxonomic Units (OTUs). The number of OTUs provides a measure of the diversity of 16S sequences in the clone library and, putatively, the bacterial diversity in the original sample. Similarly, the number of clones within each OTU provides an indication of the abundance of a group of similar sequences in the library and, putatively, the abundance of a particular organism in the sample. Phylogenetic comparison of clone sequences with 16S sequence databases provides an indication of the type of organisms represented by the sequenced clones.

The 70 RFLP profiles from the clone library cluster into 35 distinct OTUs. Twenty-nine OTUs

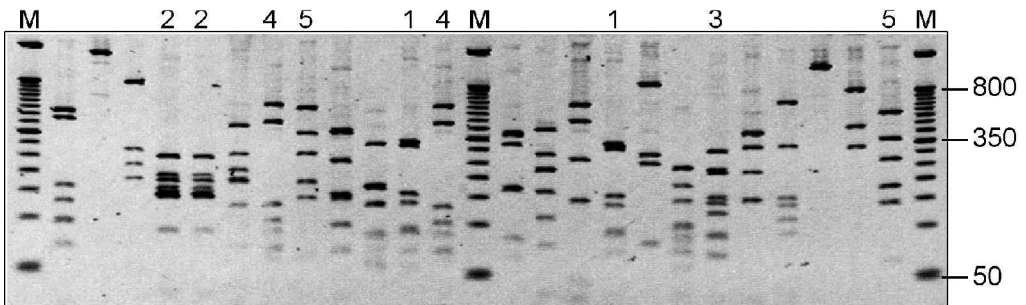


FIG. 4. Representative Restriction Fragment Length Polymorphism (RFLP) profiles obtained from the 16S clone library prepared from the discharge drain sinter sample. For the purposes of comparison, each profile type was defined as an Operational Taxonomic Unit (OTU). The numbers at the top of the figure indicate the profiles of the five dominant OTUs (OTU1–OTU5) that were represented by multiple clones in the library, and for which DNA sequence data were subsequently obtained. M denotes the molecular weight size standard (50-bp ladder, Gibco-BRL) and numbers along the side of the figure indicate size in base-pairs.

were represented by two or less clones in the library. The remaining six OTUs accounted for 38 (54%) of the RFLP profiles (see Fig. 4). The DNA sequence information was obtained from clones representing five of the six dominant OTUs (designated OTU1–OTU5). The results of the RFLP analysis and DNA sequence alignments obtained from a BLAST search of the Genbank sequence database are summarized in Table 2. No exact sequence matches were detected in the database searches although the sequence from OTU2 was nearly identical (99% similarity) to the 16S sequence of an organism described as a thermophilic and filamentous member of the green non-sulphur bacteria (GenBank accession number AB067647).

OTUs 1 and 3 aligned with groups of as-yet-uncultured organisms within the *Hydrogenophilus* grouping of the beta *Proteobacteria*, and the *Cyanobacteria*, respectively. Both OTU sequences clustered with 16S sequences obtained from thermophilic environments. However neither OTUs were very closely aligned with organisms that exist in culture therefore limiting further inferences about the likely morphology of these organisms.

The sequence representing OTU 4 was not closely related to any existing sequence but

aligned, albeit poorly, within a candidate division of environmental clone sequences (OP10) of the low G+C Gram positive bacteria. Many of the 16S sequences within this division derive from hydrothermal environments. Given the poor alignment and significant difference in sequence, OTU 4 could represent a new and as yet undescribed bacterial species. OTU 5 aligned with the *Cellvibrio* group of the gamma *Proteobacteria*. *Cellvibrio* are described as cellulolytic bacteria involved in the degradation of natural cellulosic fibres (Blackall *et al.*, 1985). There is no record of there being thermophilic members of this group.

While ARDRA analysis provides an indication of the composition of the microbial community of the sinter sample, the physical arrangement or architecture of the community remains unknown. It is hence not possible to specify which of the organisms afford a suitable substrate for the flocculating silica or, even, which are sessile and which are not.

Mineralogy

All samples showed the characteristic X-ray scattering broadband of opal-A – the dominant phase present (cf. Smith, 1998; Herdianita *et al.*,

TABLE 2. Phylogenetic affiliation of 16S sequences from dominant clone types (OTUs) with sequences in the GenBank databases.

RFLP type (OTU) ^a	Library % ^b	GenBank Accession No.	Closest relative or sequence ^c	Identity ^d	Phylogenetic grouping
1	8.6	AY222297	Uncultured <i>Hydrogenophilus</i> sp. AF402975.1 ^e	1425/1437 (99%)	β Proteobacteria
2	10.0	AY222298	Anaerobic filamentous bacteria AB067647	1397/1400 (99%)	Chloroflexi (green non-sulphur bacteria)
3	7.1	AY222299	Uncultured cyanobacterium AF4456777	1198/1258 (95%)	Cyanobacteria
4	11.4	AY222300	Uncultured bacterium AJ271048.1	1147/1244 (92%)	Candidate division OP10
5	11.4	AY222301	<i>Cellvibrio</i> sp. AJ289164.1	1397/1426 (97%)	γ Proteobacteria
6	5.6		not sequenced		
7, 8, 9	2.8 each		not sequenced		
10–35	1.4 each		not sequenced		

^a Operational taxonomic unit

^b Percentage of clones in library with the designated OTU

^c Determined from the highest scoring match in a BLAST search of GenBank database

^d Number of identical bases between the query and GenBank sequence

^e Obtained from a hot spring at Kuirau Park, Rotorua, New Zealand

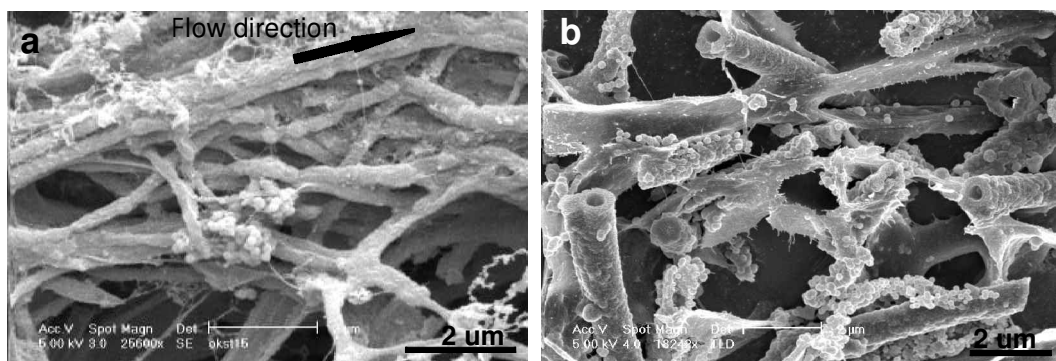


FIG. 5. SEM cryostage images of microspheres of juvenile opal-A clustering upon filamentous bacteria, Rainbow Terrace, Orakei Korako: (a) streamer fabric, AU52404; (b) bubble mat, AU52390.

2000*a,b*). Opal-A is the first silica phase to deposit and, in all cases examined, the youngest silica has flocculated upon a bacterial substrate (e.g. Fig. 5*a,b*).

In general, values of FWHM and FWTM decrease with increasing sample age (Table 1). FWHM decreases from 1.37 Å at 0.12 y old to 1.30 Å at age ~2 y, with FWTM values decreasing from 2.23 to ~2.0 Å over the same time interval. The behaviour of FWQM values is less consistent. Samples AU52387_3d and _5d, show a larger proportional decrease in FWHM

and FWTM values when compared with all other samples implying that changes occur in the opaline silica not only immediately it is removed from the parental water but also following initial deposition (cf. Iler, 1979). Overall, the halfwidth values of the Group A and B samples and the younger Orakei Korako silicas, AU52391 and AU52396*a*, lie towards the upper end of the range of the youngest samples cited by Herdianita *et al.* (2000*a*). Importantly, FWQM, FWHM and FWTM values are independent of fabric type (streamer, palisade, bubble

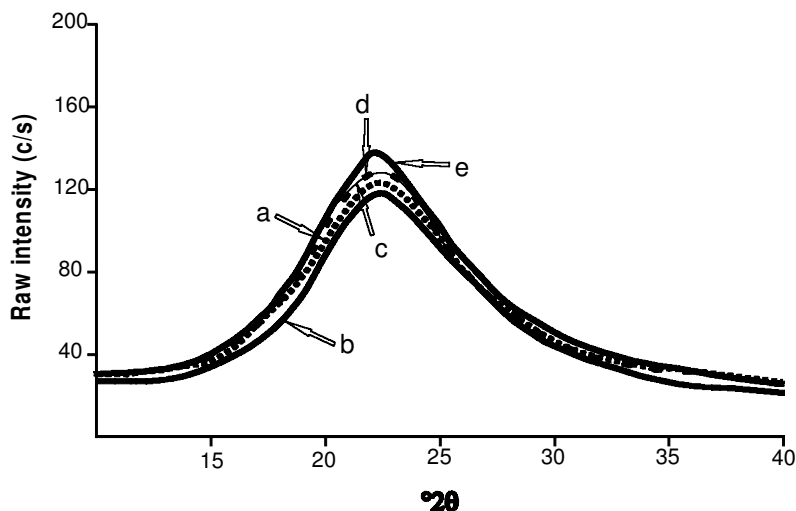


FIG. 6. Representative, smoothed, X-ray powder scattering bands for young sinters from the Wairakei Power Station discharge drain (*a–c*) and from Rainbow Terrace, Orakei Korako (*d–e*): (*a*) fresh sinter, air-dried for 6 h, <46 days old (0.12 y), AU52387*a*, maximum intensity 93 c/s; (*b*) sinter air-dried 16 days, 62 days old (0.16 y), AU52387*d*, maximum intensity 90 c/s; (*c*) sinter from the bank of the Wairakei drain, <<234 days old (<<0.5 y), AU52389*b*, maximum intensity 103 c/s; (*d*) palisade microfacies (<0.5 y), AU52396*a*, maximum intensity 104 c/s; (*e*) bubble mat microfacies (>1 and >2 y), AU52394, maximum intensity 107 c/s.

mat), being similar among all samples of more or less similar age, within experimental error.

In general, the values of maximum intensity increase with increasing age (Fig. 6, Table 1). The maximum intensities of Group A samples <0.2 y old show values <94 c/s and, apart from AU52389a, are considerably lower than all other samples. Samples from all three groups within the age range of >0.2 and <0.5 y have values of 100 ± 4 c/s. The majority of samples with an age >0.5 y show the highest maximum intensity values ranging from 106 to 112 c/s.

Silica morphology
Group A

The first-deposited silica of the Wairakei drain forms a densely-packed mat of opal-A woven

from barbichel-like filaments consisting of a coating of smooth silica presumably deposited about the living microbes. These strands are commonly aligned parallel with the flow direction (Fig. 7a), but some divaricate and criss-cross to form a weft to the main strands warp. In places, occasional strand ends protrude above the surface of the mat. Typically, individual barbichels are <8.0 μm long but some grow as large as 55 μm , and while their diameter is commonly 0.3–0.7 μm it may be up to 1.0 μm . At high magnification, >50,000 \times , the initial completed strands can be seen to be formed by agglomeration of clusters of nanospherical particles <300 nm in diameter.

With deposition of further silica, the barbichel-strands transform to become a string of juxtaposed, coalesced, oblate opal-A microspheres,

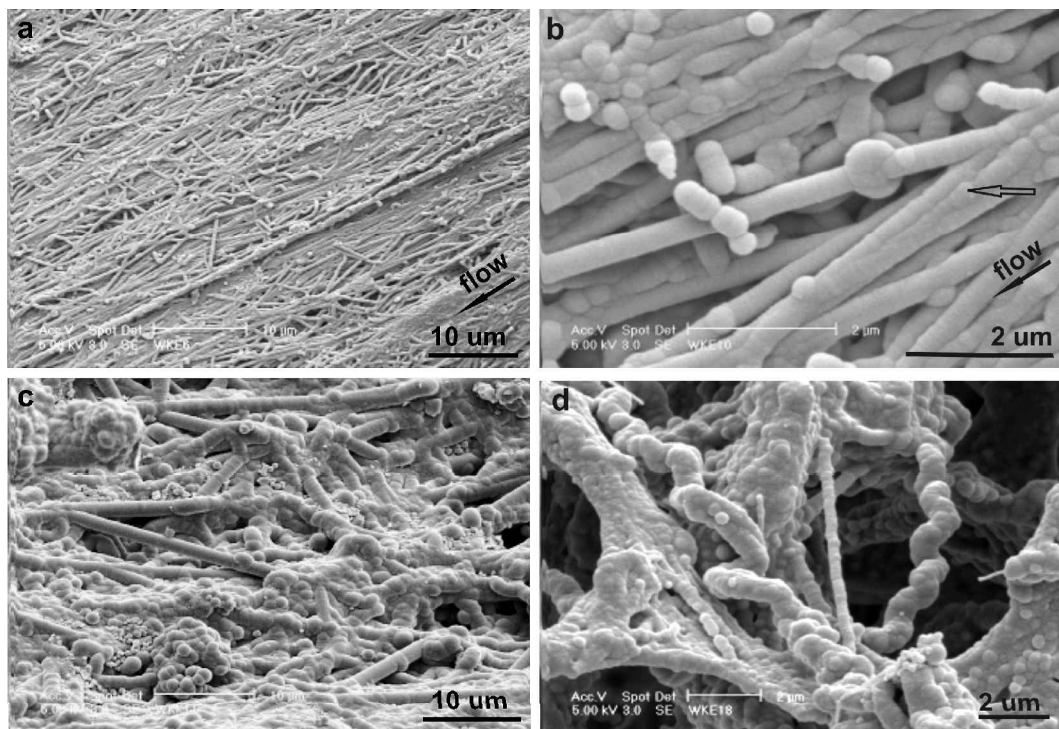


FIG. 7. SEM images of sinter, Wairakei discharge drain, (a,b,d) Group A fresh sinter, AU52387, air-dried for 3 days i.e. <49 days old; (c) Group B sinter, AU52388, ex-drain <0.4 y old: (a) densely-packed mat of silica-coated, barbichel-like strands, generally aligned with the flow direction. Some strands crisscross forming a weft to the warp of the main strands; (b) closely-packed barbichel-like silica strands transforming into strands of oblate microspheres $0.2 \times 0.4 \mu\text{m}$ (arrow). Clusters of oblate, opal-A microspheres, $0.2 \times 0.4 \mu\text{m}$, have enveloped some smooth silica strands; (c) tangled chains of oblate, coalesced spheres forming a closely-packed mat of barbichel-like strands with clusters of small ($\sim 0.4 \mu\text{m}$ diameter) late-stage (second generation) microspheres distributed on the surface; (d) twisted, clockwise, helical, silica strands such as occur in both Group A and Group B samples.

commonly $0.2 \times 0.4 \mu\text{m}$ (Fig. 7b). Only in a few of these is the underlying substructure of agglomerated nanospheres obvious. Additional silica deposition can impart an irregular and lumpy appearance to the strands (Fig. 7c). Elsewhere, a second generation of occasional, well-formed, $\sim 0.4 \mu\text{m}$ diameter, opal-A microspheres are scattered across the mat surface. Voids with a maximum size of $5 \times 2 \mu\text{m}$, commonly occur where strands divaricate at angles of up to 45° from the principal direction of strand alignment – and the direction of water flow.

Euhedral halite crystals, $< 1.5 \mu\text{m}$ along the cube edge, litter the surface of the SEM mount and presumably have crystallized from residual parent alkali chloride fluid upon air drying of the sample. Diffraction lines of halite occur in XRPD scans of all Group A but not in any Group B samples, where any traces of the parent fluid have presumably been washed out by rain.

Group B

The opal-A of these samples displays a similar habit to that of the Group A streamer microfacies. Opal-A spheres again form chains of oblate, coalesced microspheres, but the average sphere size in Group B samples is up to $1.8 \mu\text{m}$ diameter and their sphericity is more pronounced than in Group A such that the Group B strands often resemble a string of beads. In places the outlines of individual spheres that form the silica strands have become obscured by a late silica overgrowth (Fig. 7c).

As in Group A, a second generation of well-formed opal-A spheres, up to $0.5 \mu\text{m}$ across, nestle in hollows of the primary silica mat. Their occurrence indicates that silica continues to deposit after the sinter is removed from the drain, presumably from inter-pore fluid. It is among the oldest Group A and the Group B samples that a higher maximum intensity of the opal-A X-ray scattering band occurs and this increase is taken as denoting the initial maturation of the juvenile silica that occurs within the first 300 days following deposition.

Wallrock

Sample AU52389a was deposited directly on the wall of the Wairakei drain. In the horizon immediately adjacent to the drain wall (Zone 1), i.e. the oldest, closely-packed silica strands are aligned both with one another and the flow direction; the close-packing of the silica strands

giving the sinter its coherency. An undulating and gradational contact occurs between this wall-attached layer and the next silica layer out from the wall (AU52389b, Zone 2) which varies in thickness from 2–10 mm. Silica in this second horizon also occurs in strands but these lack preferred orientation. There is no cementation between them. They are bound together by numerous intertwining and overlaps. Beyond Zone 2, the sinter again takes on the typical streamer fabric appearance aligned with the flow direction (Zone 3). Individual main central strands are up to 50 mm long.

These drain samples indicate the profound effect that current flow can exercise on the habit of streamer microfacies sinter (Fig. 8). Initially, along the newly-cleaned relatively-flat drain surface, the hydrodynamics of the drain produce a thin laminar sublayer in the moving fluid (cf. Blatt *et al.*, 1980). Bacteria populating this sublayer produce strands (filaments) aligned and oriented more or less with the main flow direction. Silica deposited upon them adopts the habit of the microbial template (Zone 1). Any irregularities in Zone 1 that project through the laminar flow sublayer can shed eddies into the main flow. Differential silica deposition in and around these eddies will yield the undulations seen in the gradational contact between Zones 1 and 2 and produce a surface that is hydrodynamically rough and, in turn, generating a turbulent sublayer within the flow pattern. Few microbial strands that grow in this sublayer would be expected to be oriented with respect to the main flow direction, nor would any silica moulds that

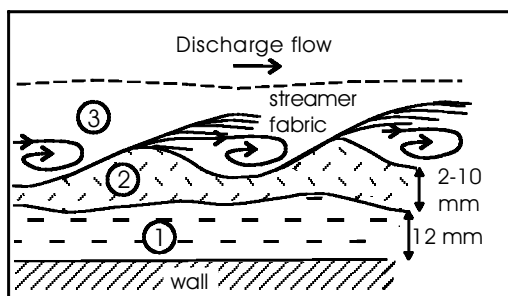


FIG. 8. Schematic interpretation of the effect of turbulence on microbial growth habit and silica deposition in Wairakei discharge drain. Zone 1: initial sinter substrate. Zone 2: secondary substrate that both results from and causes local turbulence. Zone 3: silica strands piercing turbulent sublayer, largely aligned with and flexing in main flow.

might form about them (Zone 2). The pronounced, undulating contact between Zones 2 and 3 resembles that produced during deposition in turbulent fluid such as is commonly developed downstream of ripples (cf. Blatt *et al.*, 1980). It is in this zone, presumably, that helical strands of silica could grow. However, a number of bacteria (e.g. Spirochetes) are known to exhibit a spirillum-like morphology akin to that illustrated in Fig. 7d irrespective of flow environment (Holt *et al.*, 1993). Insofar, as the velocity gradient in turbulent flows is steeper close to the channel wall than in the channel centre, turbulence has least effect on the flow away from the rough wall, and hence on the structure of any potential microbial substrate growing in this zone, that, in turn, could influence the habit of the silica depositing here. As individual microbial strands grow they eventually penetrate the turbulent sublayer and emerge into the main (laminar) current. This occurs in the Wairakei drain, once strands exceed 22 mm. It is at this point that the strands of streamer fabric again evolve parallel to the principal flow direction (Zone 3).

Group C

Opal-A spheres in the >1 and <2 y old sinter of Orakei Korako Group C samples possess the habits typical of those found in innumerable young sinters where silica has deposited upon a microbial substrate (e.g. Herdianita *et al.*, 2000a; Rodgers, 2000). Well-formed, opal-A spheres, <1 μm in diameter, are commonly observed coalesced about microbial filament templates

(Fig. 9). Elsewhere, individual microspheres occur in botryoidal clusters. The proportion of well-formed opal-A spheres increases with increasing age.

Discussion

Molecular community analysis provides the opportunity to gain new insights into the nature of microbial communities that are typically recalcitrant to analysis by culture-based methods. The 16S sequences detected in this study did not exactly match those of named organisms, and hence the specific identification and further characterization of organisms present in the sample was not possible, nor can specific DNA profiles be associated with potential microbial silica substrates. Similar difficulties were encountered by Inagaki *et al.* (2001) in providing a comprehensive analysis of the complex bacterial community of Steep Cone hot spring, Yellowstone. However the phylogenetic placement of the Wairakei sequences provides a strong basis for inferring the diversity of organisms present and in some cases their physiological properties.

Preliminary attempts to PCR amplify 16S sequences using *Archaea*-specific primers were unsuccessful. This does not necessarily indicate the absence of *Archaea* in the sample as it is possible that the primers did not match the organisms present. Use of more extensive primer sets and *in situ* hybridization with domain-specific probes could have been used to

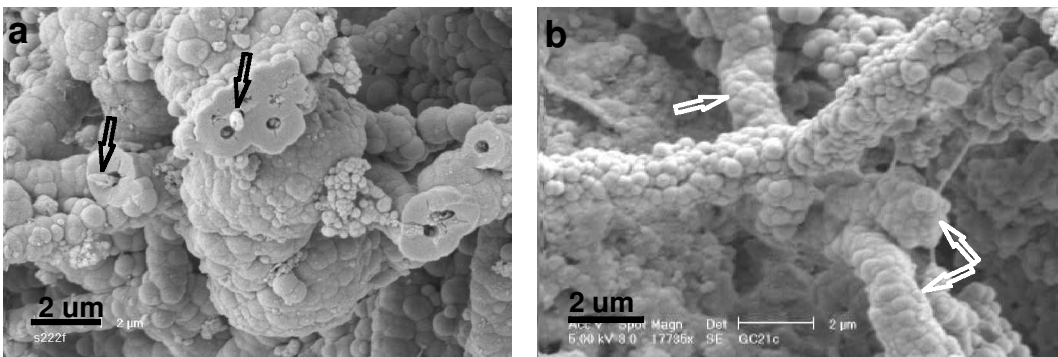


FIG. 9. SEM images of young sinter, <2 y old, exhibiting typical juvenile habits, Orakei Korako: (a) coalescence of opal-A microspheres <1.0 μm in diameter, to form a mould about silicified microbial trichomes (arrowed), AU52393; (b) AU52392a, newly-formed opal-A microspheres <0.5 μm in diameter forming botryoidal clusters on filaments. Some filaments display coalesced, oblate opal-A spheres (arrowed) similar in habit to those in Fig. 7.

validate the results although such work was beyond the limited resources of the current study.

The RFLP analysis of the Wairakei sinter sample suggests that the bacterial community is moderately diverse, but is dominated by five major groups of organisms, present in approximately equal proportions, that account for approximately half of the community. On the basis of phylogenetic inference, it is probable that at least one of these dominant groups of organisms, represented by OTU 2, are filamentous bacteria, and that three others (OTUs 1, 3, 4) are thermophilic. The results of the molecular analysis are therefore consistent with the thermophilic environment from which the sample was collected and ultrastructural observations by SEM of the sinter samples which indicate a significant abundance of filamentous templets.

However, the types of organisms detected in this study clearly differ from the results of the similar studies by Inagaki *et al.* (1998, 2001) which indicated an abundance of *Thermus* and *Hydrogenobacter* spp in sinter-associated assemblages from Yellowstone National Park and a geothermal power plant in Japan. None of the clone sequences obtained in our study clustered within these groups. While it is possible that this is due to subtle methodological differences in the extraction and analysis of microbial DNA from samples, it is more likely that these differences reflect the effect of different temperatures on the microbial community structure. The temperature recorded at our sample site was 62.5°C while the sinter samples examined by Inagaki *et al.* (2001) were collected from sites with higher temperatures ranging from 75 to 85°C. It is also possible that there are biogeographic differences in the sinter communities as the sequence for OTU1 was most closely related to a 16S sequence that was obtained from a hydrothermal pool in Kuirau Park, Rotorua, New Zealand (Sunna and Bergquist, 2001) suggesting that this is a locally prevalent organism.

Some caution must be applied in the interpretation bacterial abundance based on OTU data as the processes of DNA extraction, PCR amplification and clone library construction may all bias the ratio of organisms detected. Nevertheless the information obtained in this study provides the basis for preparation of taxon-specific probes that can be used in combination with direct microscopic methods to confirm the abundance of organisms detected by this study. Such future studies will also enable

more information to be obtained on the morphology of these organisms and their physical arrangement within the sinter fabric. An indication of the types of organisms present in the samples also provides valuable information on the possible culture conditions needed to isolate representative organisms from these environments.

The detection of 16S sequences in this study that are most closely related to clone sequences derived from thermophilic environments elsewhere supports the notion that these environments comprise a distinctive bacterial community that is poorly characterized. (Inagaki *et al.*, 2001). Importantly, the dominance of sequences that represent clades of as-yet uncultured organisms further reinforces the observation that culture-based studies do not provide an accurate representation of the microflora in these environments.

Difficulties exist in endeavouring to ascribe specific silica sinter textures to biogenic or abiogenic processes (cf. Inagaki *et al.*, 2001). However, the deposition and development of opal-A and the ensuing changes observed in the crystal chemistry and texture following deposition and subsequent removal from its parent fluid, are consistent with what is known of the behaviour of silica in both natural and abiogenic laboratory systems of comparable pH, temperature and dissolved salt content to the Wairakei and Orakei Korako parent fluids. At both localities several distinct stages of silica deposition are involved: (1) silica nanospheres flocculate from the sol phase and agglomerate as microspheres; (2) the microspheres settle on suitable substrates, including bacteria, and grow in number and size; (3) the original bacteria become silicified; (4) secondary microspheres form and settle on substrates; (5) silica overgrowths obliterate the outlines of the juvenile textures.

For silica to flocculate from the Wairakei discharge water under the prevailing pH and temperature conditions, the presence of other agents such as dissolved Ca²⁺ and Na⁺ or microbes would appear to be essential. Above a pH of 6, pure silica sols are relatively stable. All silica particles, including oligomers, bear a negative charge and mutually repel one another. With increasing pH, there is a decrease in the number of interparticle collisions, and hence in opportunities for adhesion and growth (Iler, 1979). Coagulation, i.e. growth of such particles that may lead to flocculation, occurs readily

where particle-particle interaction is afforded by residual bonds or some other form of particle-particle bridging. This can occur in the presence of coagulants such as salt cations or organic molecules. Iler (1979, p. 376) states that, “in all cases, flocculation is due to interparticle bonding through the cations”. He illustrates this with specific reference to the role that Na⁺ can play (Fig. 4.17a, p. 377), arguing that coagulation can occur as soon as sufficient ion-exchanged Na⁺ has been absorbed on to the surface of each silica particle. Given their similar silica levels, Wairakei 480 µg/g and Orakei Korako 400 µg/g, it is presumably the elevated salinity level in the Wairakei discharge fluids (Na⁺ 930 µg/g, Ca²⁺ 12 µg/g, Cl 1500 µg/g, pH 8.3), along with its high microbial content, that facilitates flocculation and rapid build up of the opaline silica in the drain despite the high pH (~8.3) and water temperature (~60°C) that favour gelling. In contrast, at Orakei Korako where the parent fluid is dilute (Na⁺ 180 µg/g, Ca²⁺ 0.2 µg/g, Cl 400 µg/g, pH 8.1) and discharge levels markedly lower, sinter grows more slowly, particularly distal from the vent on the sinter aprons.

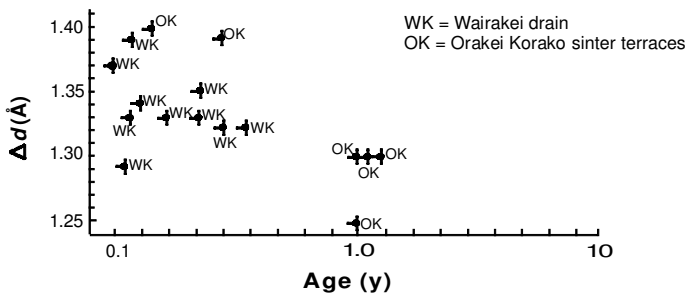
Subtle variations in dissolved salt concentration, pH, temperature and the presence or absence of organic/biological molecules determine whether the coagulum gels or develops as a solid phase (e.g. Iler, 1979, pp. 364–407). Typically, silica colloids are <5 nm in diameter. As they aggregate, the radius of curvature increases and the surface of the growing particle fills where small colloid particles adhere to a surface rather than one another. It is an extension of this process that can produce the microsphere structure and nanosphere substructure of the juvenile Wairakei silica strands.

All samples examined show a limited range in particle size and shape. Once silica particles grow

to a certain size, there is very little change in energy content with surface area and there is an optimum upper limit on the size to which particles may grow, at least in the initial stages of deposition (Iler, 1979). Further, when the growth process continues, following adhesion, larger particles grow at the expense of smaller and the latter are consequently eliminated. The two processes, acting in tandem, produce a limited size range in the microsphere end product.

Insofar as deposition occurs preferentially upon those surfaces having minimum radius, such as where two particles are in contact (Iler, 1979), a continuum of textures becomes possible as is seen in the Wairakei samples: individual oblate microspheres → juvenile strands → bead strings → irregular lumps. Growth continues readily wherever an aqueous film is present on the sinter surface such as may be supplied by pore water, either thermal or rainwater, in the case of Group B samples. This film allows activity gradients to become established and maintained that can promote the movement of silica (Landmesser, 1995). Importantly, unlike other metal oxides, solid silica remains non-crystalline throughout and enjoys an appreciable solubility in water that facilitates post-depositional growth and textural changes. The efficacy of the silica deposition process and the strength of the residual bonds that link the microspheres is reflected in the rapid build up of silica on all available surfaces throughout the Wairakei drain, despite the comparative high speed and turbulence of the discharge water.

The variations observed in the size and shape of the X-ray scattering broadband are consistent with established models of behaviour in young non-crystalline silicas. When first removed from its parent fluid, opaline silica loses water and its juvenile, open structure collapses (Iler, 1979).



Presumably it is this change that is reflected in the initial reduction in FWQM, FWHM and FWTM and the changes in scattering intensity. Subsequently, as the scattering intensity increases and the half widths decrease further, if, as in clays, the half width is taken as a measure of lattice disorder, then a small reduction in the disorder of the opaline structure is implied during the earliest maturation of the deposit. Certainly, the half width changes observed in the present study are consistent with the pattern of behaviour found by Herdianita *et al.* (2000a) who reported an overall decrease in FWHM with time. The results presented here extend the range of their aging model, plotting in the lower part of the range of their year-1 values (Fig. 10). Whatever, the precise nature of the processes involved, the evidence points to substantial post-depositional structural and textural changes occurring at a very early stage in opaline silica. Hence, samples collected from extinct hot springs or even modern depositing springs have experienced substantial textural and silica phase modification. The evidence suggests that even specimens stored in museum collections have been subject to an indeterminate amount of change and questions the extent to which their mineralogy and textures might be used to elucidate details of the original depositional process or, perhaps, the specifics of the microbes involved.

Acknowledgements

Thanks are due to Contact Energy for allowing access to and sampling of the Wairakei Power Station discharge drains and to Ruth Smith and Lew Bacon for supplying additional information. Phillipa and Craig Gibson granted access to and allowed sampling of the sinter terraces at Orakei Korako. KAR received funding from the University of Auckland Research Committee and BYS from Environment Waikato and the Jeff Allen Memorial Fund of the University of Auckland.

References

- Altschul, S.F., Gish, W., Miller, W., Myers, E.W. and Lipman, D.J. (1990) Basic local alignment search tool. *Journal of Molecular Biology*, **215**, 403–410.
- Amann, R.L., Ludwig, W. and Schleifer, K.H. (1995) Phylogenetic identification and in situ detection of individual microbial cells without cultivation. *Microbiological Reviews*, **59**, 143–169.
- Blackall, L.L., Hayward, A.C., Sly, L.I. (1985) Cellulolytic and dextranolytic Gram-negative bacteria: revival of the genus *Cellvibrio*. *Journal of Applied Bacteriology*, **59**, 81–97.
- Blank, C.E., Pace, N.R. and Cady, S.L. (1999) A molecular biogeographic comparison of microbial communities in near boiling silica-depositing Yellowstone thermal springs; relating communities to siliceous sinter textures. *Geological Society of America Annual Meeting, Denver Colorado, Abstracts with Programs* **31**(7), 325.
- Blatt, H., Middleton, G. and Murray, R. (1980) *Origins of Sedimentary Rocks* 2nd edition. Prentice-Hall, New Jersey, USA.
- Brosius, J., Dull, T.L., Sleeter, D.D. and Noller, H.F. (1981) Gene organisation and primary structure of a ribosomal RNA operon from *Escherichia coli*. *Journal of Molecular Biology*, **148**, 107–127.
- Cady, S.L. and Farmer, J.D. (1996) Fossilization processes in siliceous thermal springs: trends in preservation along thermal gradients. Pp. 150–173 in: *Evolution of Hydrothermal Ecosystems on Earth (and Mars?)*. Ciba Foundation Symposium, Wiley, Chichester, UK.
- Farmer, J.D. (2000) Hydrothermal systems: doorways to early biosphere evolution. *GSA Today*, **10**, 1–9.
- Herdianita, N.R., Browne, P.R.L., Rodgers, K.A. and Campbell, K.A. (2000a) Mineralogical and morphological changes accompanying aging of siliceous sinter and silica residue. *Mineralium Deposita*, **35**, 48–62.
- Herdianita, N.R., Rodgers, K.A. and Browne, P.R.L. (2000b) Routine procedures for characterising modern and ancient silica sinter deposits. *Geothermics*, **29**, 65–81.
- Holt, J.G., Krieg, N.R., Sneath, P.H.A., Staley, J.T. and Williams, S.T. (editors) (1993) *Bergey's Manual of Determinative Bacteriology* 9th edition. Williams and Wilkins, Maryland, USA, 787 pp.
- Hugenholtz, P., Pitulle, C., Hershberger, K.L. and Pace, N.R. (1998) Novel division level bacterial diversity in a Yellowstone hot spring. *Applied and Environmental Microbiology*, **180**, 366–376.
- Iler, R.K. (1979) *The Chemistry of Silica: Solubility, Polymerization, Colloid and Surface Properties, and Biochemistry*. Wiley-Interscience, New York, 866 pp.
- Inagaki, F., Hayashi, S., Doi, K., Motomura, Y., Izawa, E. and Ogata, S. (1997) Microbial participation in the formation of siliceous deposits from geothermal water and analysis of the extremely thermophilic bacterial community. *FEMS Microbiology Ecology*, **24**, 41–48.
- Inagaki, F., Yokoyama, T., Doi, K., Izawa, E. and Ogata, S. (1998) Bio-deposition of amorphous silica by an extremely thermophilic bacterium *Thermus* spp.

- Bioscience, Biotechnology and Biochemistry*, **62**, 1271–1272.
- Inagaki, F., Motomura, Y., Doi, K., Taguchi, S., Izawa, E., Lowe, D.R. and Ogata, S. (2001) Silicified microbial community at Steep Cone Hot Spring, Yellowstone National Park. *Microbes and Environments*, **16**, 125–130.
- Landmesser, M. (1995) Mobilität durch Metastabilität: SiO₂ Transport und Akkumulation bei niedrigen Temperaturen. *Chemie der Erde*, **55**, 149–176.
- Lloyd, E.F. (1972) Geology and hot springs of Orakeikorako. *New Zealand Geological Bulletin*, **85**, 1–164.
- Miller, D.N., Bryant, J.E., Madsen, E.L. and Ghiorse, W.C. (1999) Evaluation and optimization of DNA extraction and purification procedures for soil and sediment samples. *Applied and Environmental Microbiology*, **65**, 4715–4724.
- Rodgers, K.A. (2000) Research on silica sinters. *Mineralogical Society Bulletin*, **126**, 16–17.
- Sambrook, J. and Russell, D.W. (2001) *Molecular Cloning: A Laboratory Manual*, **1-3**, 3rd edition. Cold Spring Harbor Laboratory Press, New York.
- Smith, D.K. (1998) Opal, cristobalite, and tridymite: noncrystallinity versus crystallinity, nomenclature of the silica minerals and bibliography. *Powder Diffraction*, **13**, 2–19.
- Sunna, A. and Bergquist, P.L. (2001) A gene encoding a novel extremely thermostable 1,4-beta-xylanase isolated from an environmental DNA sample from Kuirau Park, Rotorua, New Zealand. GenBank Accession number AF402975.
- Weed, W.H. (1889a) On the formation of siliceous sinter by vegetation of thermal springs, *American Journal of Science*, **37**, 351–359.
- Weed, W.H. (1889b) Formation of travertine and siliceous sinter by the vegetation of hot springs. *US Geological Survey 9th Annual Report, 1887–1888*, 613–676.

[Manuscript received 8 August 2002;
revised 6 February 2003]